

## Research Article

# Anticancer and Antibacterial Activity of Cadmium Sulfide Nanoparticles by *Aspergillus niger*

Mohammed S. Alsaggaf,<sup>1</sup> Ashraf F. Elbaz,<sup>2</sup> Sherin El Badawy,<sup>2</sup> and Shaaban H. Moussa<sup>1,2</sup> 

<sup>1</sup>College of Science and Humanitarian Studies, Shaqra University, Qwaieah 11971, Saudi Arabia

<sup>2</sup>Genetic Engineering and Biotechnology Research Institute, University of Sadat City, Egypt

Correspondence should be addressed to Shaaban H. Moussa; shaus2008@yahoo.com

Received 12 March 2020; Accepted 7 May 2020; Published 8 June 2020

Academic Editor: Yohei Kotsuchibashi

Copyright © 2020 Mohammed S. Alsaggaf et al. This is an open access article distributed under the Creative Commons Attribution License, which permits unrestricted use, distribution, and reproduction in any medium, provided the original work is properly cited.

Cadmium-tolerant (6 mM) *Aspergillus niger* (RCMB 002002) biomass was challenged with aqueous cadmium chloride (1 mM) followed by sodium sulfide (9 mM) at 37°C for 96 h under shaking conditions (200 rpm), resulting in the formation of highly stable polydispersed cadmium sulfide nanoparticles (CdSNPs). Scanning electron microscopy revealed the presence of spherical particles measuring approximately 5 nm. A light scattering detector (LSD) showed that 100% of the CSNPs measure from 2.7 to 7.5 nm. Structural analyses by both powder X-ray diffraction (XRD) and Fourier transform infrared spectroscopy (FTIR) confirmed the presence of cubic CdS nanoparticles (CdSNPs) capped with fungal proteins. These CdSNPs showed emission spectra with a broad fluorescence peak at 420 nm and UV absorption onset at 430 nm that shifted to 445 nm after three months of incubation. The CdSNPs showed antimicrobial activity against *E. coli*, *Pseudomonas vulgaris*, *Staphylococcus aureus*, and *Bacillus subtilis*, and no antimicrobial activity was detected against *Candida albicans*. The biosynthesized CdSNPs have cytotoxic activity, with 50% inhibitory concentrations (IC<sub>50</sub>) of 190  $\mu\text{g mL}^{-1}$  against MCF7, 246  $\mu\text{g mL}^{-1}$  against PC3, and 149  $\mu\text{g mL}^{-1}$  against A549 cell lines.

## 1. Introduction

The use of various toxic substances and the higher energy consumption arising in various chemical and physical processes hinder their extensive field applications. Notably, the microbial biosynthesis of metal nanoparticles emerged as a significant branch of nanobiotechnology because it is cost-effective, ecofriendly, and unlike other physical and chemical processes. These nanoparticles are also size-reproducible and more monodisperse and have greater stability than synthetically produced ones [1].

The benefits of using microorganisms to develop efficient methods for synthesizing quantum dots compared with other biological objects is their capabilities to function in an environment under stressful conditions, particularly in the presence of high metal concentrations as well as sudden changes in the pH, temperature, and pressure [2].

The capabilities of microorganisms to produce green Cd-containing nanocrystal were attributed to its ability to resist heavy metals via the bioreduction and precipitation of

soluble metallic ions, producing insoluble nanometric complexes [3]. In bacteria, the biosynthesis of intracellular CdSNPs can be distinguished in *Thermoanaerobacter* sp. [4], *Klebsiella pneumoniae* (5 to 200 nm) [5], and *Escherichia coli* (2 to 5 nm), [6] and also the extracellular biosynthesis in *Klebsiella aerogenes* (20 to 200 nm) [7], *Rhodopseudomonas palustris* (8 nm) [8], *Clostridium thermoaceticum* [9], *Rhodobacter sphaeroides*, *Serratia nematodiphila* [10], *Shewanella oneidensis* [11], *Gluconacetobacter xylinus* (30 nm) [12], and *Lactobacillus* sp. [13], and intra- and extraspherical NPs measuring 40~50 nm by *Desulfovibrio caledoiensis* and *Enterococcus* sp. (50 to 180 nm) [14].

The usage of eukaryotic microorganisms is potentially exciting since they secrete high levels of proteins and enzymes, thus increasing yield, and they are simple to manage in the laboratory and at an industrial scale. Because of their tolerance and their bioaccumulation ability of metals, fungi are an attractive center stage in biological group generation of metal nanoparticles. Few advantages of using a fungal-mediated green approach to the nanoparticle synthesis

are as follows: economic capability and ease in scale-up and handling, thus making it possible to obtain biomass easily for processing, and large-scale production of different extracellular enzymes [15]. It has been reported that five yeast strains, namely, *Candida glabrata* for hexamers that are intracellularly and extracellularly synthesized [16], *Candida glabrata* for intracellularly synthesized compounds [17], *Schizosaccharomyces pombe* [6–8, 17], *Trichosporon jirovecii* [18], and *Saccharomyces cerevisiae* [19], can produce CdSNPs when cultured within the presence of cadmium salts. CdSQD nanoparticles were also extracellularly biosynthesized by *Fusarium sp. ciceris* [20] that adhered to the cell wall [21] via *Fusarium oxysporum* and from a *Fusarium oxysporum* f. sp.-*lycopersici* 4287 [22] mycelium mat. *Trichoderma harzianum* [23], *Pleurotus ostreatus* [24], and *Phanerochaete chrysosporium* [25] could also biosynthesize CdSNPs, whereas the white rot fungus *Corioliolus versicolor* has been capable of synthesizing CdSQDs without the use of an external source of sulfur [26].

The development of novel cadmium-based quantum dots shows great potential in the treatment and identification of cancer and targeted drug delivery due to their better size, highly optical fluorescence property, and ease to functionalize the tissue [27].

In the present work, the biosynthesis of CdSNPs by *Aspergillus niger* is reported for the first time, in which *Aspergillus niger* biomass was challenged with aqueous cadmium chloride (1 mM) and sodium sulfide (9 mM) at 37°C for 96 h under shaking conditions (200 rpm), resulting in the formation of high stable CdS nanoparticles. These CdSNPs were screened against different microbes and against different cancer cell tissues.

## 2. Material and Methods

**2.1. Microorganism.** The fungus *Aspergillus niger* (RCMB 002002) was subjected to 6 mM cadmium nitrate and maintained on PDA (potato 20% w/v, dextrose 2% w/v, and agar 2% w/v) slants. The *Aspergillus niger* spores of four-day-old slants were inoculated with a concentration of  $4 \times 10^6$  spores L<sup>-1</sup> into 250 mL flasks having 100 mL of medium MGYD which consists of yeast extract 0.3% w/v, glucose 1.0% w/v, malt extract 0.3% w/v, and peptone 0.5% w/v. Then, the flasks were incubated in the incubator-shaker for 5 days at 30°C and 150 rpm. All experiments were performed in duplicate and repeated twice, and the results are reported with their associated standard errors.

**2.2. Biosynthesis of Nanoparticles.** After the end of five days of the incubation period, the fungal mycelia were collected by filtration using filter paper No. 1 and washed with twice-distilled water three times. To initiate nanoparticle biosynthesis, three grams of mycelia was suspended in 75 mL of CdCl<sub>2</sub> (1 mM), which was shaken for 20 min. at 30°C, and then, Na<sub>2</sub>S (9 mM) was added and left for 5 days. The biomass was filtered and washed with bidistilled water three times, then suspended in 10 mL and sonicated for 10 minutes. The sonicated samples were then centrifuged at 6000 × g for 15 min to remove the cell debris, and the supernatant was

collected and filtered through a filter membrane for further characterization experiments.

**2.3. Characterization of Nanoparticles.** For all the samples, the UV-Vis spectra from 200 to 600 nm were measured by a Shimadzu UV-1800 (Japan) spectrophotometer against the cell with distilled water as a reference. The emission spectra were determined using a fluorescence spectrophotometer (Jobin-Yvon Horiba FluoroMax-4, HORIBA, Ltd., Japan) with  $\lambda_{exc}$  of 360 nm.

The formation of CdS nanoparticles was determined by X-ray diffraction (XRD) techniques using an X-ray diffractometer (X'Pert Pro, PANalytical, Netherlands) with Cu-K radiation ( $k = 1.5405 \text{ \AA}$ ) with a wide range of Bragg's angles ( $20^\circ \leq 2\theta \leq 60^\circ$ ). In addition, the FTIR spectra (Fourier transform infrared spectra) were determined by Bruker Tensor 27 (USA). The elemental composition of the sample was characterized by using energy-dispersive X-ray (EDS) analysis (Seron AIS 2300, Korea). Furthermore, the morphology and the average size of nanoparticles were determined using a transmission electron microscope (TEM, Philips CM20). Zetasizer ver. 6.32 DLS (Malvern Instruments Ltd.) was used to determine the particle sizes.

**2.4. Antimicrobial Activity.** Antimicrobial susceptibility testing was carried out by the standard well diffusion method [28] against four bacteria (*Proteus vulgaris* ATCC 13315, *Escherichia coli* ATCC 25955, *Bacillus subtilis* NRRL B-543, and *Staphylococcus aureus* RCMB010010) and one yeast (*Candida albicans* ATCC 10231). The bacterial cultures were grown in Luria-Bertani (LB) broth media, and the yeast strain was grown in yeast malt broth for 24 h. After that, 100  $\mu$ L ( $10^5$  CFU/mL) of the bacterial and yeast cultures was spread uniformly on the LB and yeast malt agar plates, respectively, and wells (8 mm) were pricked using a sterile cork borer. Then, the wells were filled with a fixed volume of the CdSNPs and water as a control. The plates were placed in a refrigerator (5–10 min) for successive diffusion, and subsequently, the bacterial strains were incubated at 37°C for 24 h, and the fungal strains were incubated for 48 h at 30°C. After the incubation, the diameter of the inhibition zone was determined and recorded. The experiments were performed in triplicate, and therefore, the average diameter of the inhibition zone with its standard deviation was determined.

**2.5. In Vitro Cytotoxicity.** The anticancer efficacy of the biosynthesized CdNPs was evaluated in terms of their *in vitro* cytotoxicity against breast cancer (MCF7), human lung cancer, non-small-cell carcinoma (A549), and prostatic small cell carcinoma (PC3), which were estimated by a methylene blue assay. The cell lines were cultured in a 96-well plate in Dulbecco's adjusted Eagle's medium (DMEM) (10,000 cells/well/100  $\mu$ L) containing 10% heat-inactivated fetal bovine serum, gentamycin (50  $\mu$ g/mL), and 1% L-glutamine to adhere the cells under appropriate conditions (37°C, 5% CO<sub>2</sub>) for 24 h. A series of twofold dilutions of the examined nanoparticles of cadmium sulfide were added to confluent cell monolayers, and three wells were used for each dilution and further incubated for 24 h. The controls were incubated

without the nanoparticles, with or without dimethyl sulfoxide (DMSO). After the incubation time, the media were aspirated and crystal violet solution (1%) was added to all wells for 30 seconds [29]. The plates were washed to remove the excess dye, and then, glacial acetic acid (30%) was then added and mixed thoroughly. The absorbance for each well was determined at 490 nm, and the readings were corrected against the absorbance of the wells without added stain. The relation between the cell survival and the concentrations of cadmium sulfide nanoparticle was plotted to obtain the survival curve and to calculate the 50% inhibitory concentration (IC50).

### 3. Results and Discussion

The biological synthesis of nanoparticles is believed to involve free amino acids, soluble proteins, enzymes, flavonoids, terpenoids, phenolic compounds, tannins, proanthocyanidins, carbohydrates, and vitamins [30]. Fungal systems are effective at the synthesis of extracellular nanocrystal CdS as they contain sulfate reductase enzymes that reduce the sulfate groups of the metal salts directly into the culture medium, leading to the formation of extracellular CdS nanoparticles. In addition, these fungi have a high level of enzyme synthesis and secretion also as high protein and carbohydrate compound production [31].

**3.1. UV Spectrum.** The CdSNP biosynthesis by the *Aspergillus niger* was indicated by a color change in the reaction mixture, to yellow, after the addition of sodium sulfide (Figure 1(a)). The cadmium sulfide biosynthesis was further confirmed by the UV-Vis absorption spectrum (Figure 1(b)). The CSNP sample showed a broad absorption onset at 430 nm, which was attributed to the CdSNP-surface plasmon excitation bands (Figure 1(d)) [32]; it exhibited a blue shift compared with 512-515 nm of the bulk cadmium sulfide [33] as direct evidence of the CdS nanoparticle formation with small particle sizes [34] within the presence of a capping agent, which prevented the aggregation of the nanoparticles into a bulk material [35]. Similarly, UV absorbances of the biosynthesized cadmium sulfide nanoparticles from *E. coli*, *Bacillus licheniformis*, *Pseudomonas aeruginosa*, *Fusarium oxysporum*, *Aspergillus terreus* [36], *Serratia nematodiphila* [10], the freshwater alga *Chlamydomonas reinhardtii* [37], *Escherichia coli* PTCC 1533, and *Klebsiella pneumoniae* PTCC 1053 [38] were shown at 465 nm, 459 nm, 465 nm, 468 nm, 428 nm, 420 nm, 430 nm, and 400-450 nm, respectively. The absorbance peak that occurred at 273 nm accounts for the presence of aromatic amino acids containing protein molecules as reported by [39]. This finding may confirm the presence of proteins and their possible role in the formation of the nanoparticles.

Following Mie's theory, nanoparticles with sphere shape will give one single SPR band, while nanoparticles differently shaped, i.e., rods, triangles, and cuboids, will lead to two or more SPR bands [40]. Accordingly, the biosynthesized CdNPs in the present study consisted of only a single population of spherical nanoparticles.

One of the major characteristics required for any type of the nanoparticle to be put to good use is its stability at the

room temperature. As clearly indicated in Figure 1(c), there was a slight shift in the absorption peak of the freshly prepared CdSNPs from 430 nm to 445 nm for samples stored for three months. Slight aggregation was taking place while the CdSNPs were stored over a three-month period with a disappearance in the peak at 273 nm which disappeared in the stored sample, which might be attributed to indicating the complete protein lysis in the sample.

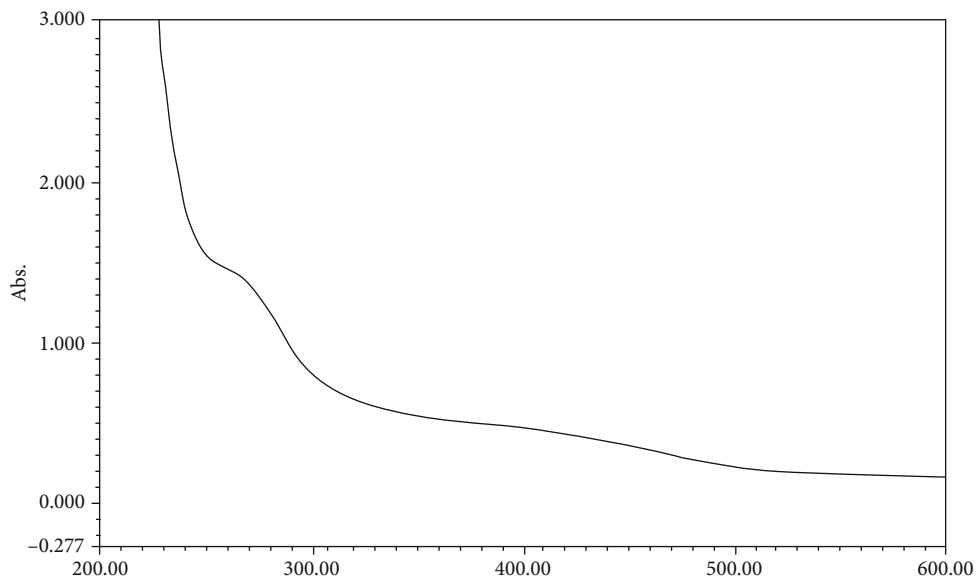
**3.2. Photoluminescence.** The fluorescence emissions of semiconductor nanoparticles are generally due to the contributions from the recombination of exciton, which usually happened at the absorption edge and owing to release emissions from the trapped deficiencies [41]. Figure 1(d) illustrates the photoluminescence (PL) spectrum of the cadmium sulfide nanoparticles that were excited at 360 nm. The nanoparticles showed one major peak at 420 nm that would correspond to emissions of the band edge. The blue shift in the emission peak was explained by the quantum confinement of the exciton because of the decreases of particle size. The slight heterogeneity of particle size was the reason of relative broadness of the emission peak width. The absence of appreciable emissions at longer wavelengths (500-700 nm) was attributed to the surface traps indicated by the absence of defect-related emissions as detected from the spectrum. This finding could be attributed to the surface modifications of nanoparticle caused by the fungal biomolecules that stabilize and develop the photoluminescence intensity.

**3.3. FTIR.** Several vibration bands of the CdSNPs biosynthesized can be observed from 4000 to 500  $\text{cm}^{-1}$  (Figure 2). In the higher energy region, the absorption peaks located at approximately 3435  $\text{cm}^{-1}$  can be assigned to the stretching vibrations of N-H, which may overlap with the O-H bond in the carboxyl group [42] owing to the amide linkages of the proteins and amino acid residues in the polypeptides [8]. The O-H bond of the carboxyl group has a peak at 2923.65  $\text{cm}^{-1}$ . Two prominent peaks at 1631  $\text{cm}^{-1}$  and 1562  $\text{cm}^{-1}$  are related to the stretching vibrations in the primary and secondary amides of the proteins, respectively [25]. The bands observed for the C-N bond at 1408- $\text{cm}^{-1}$  CdSNP  $\text{cm}^{-1}$  and 1087- $\text{cm}^{-1}$  correspond to the stretching vibrations of the aromatic and aliphatic amines, respectively. The peak located at 624.37  $\text{cm}^{-1}$  is assigned to the out-of-plane wagging of the N-H bond. The FTIR spectral results showed the possible interactions of the CdS nanoparticles with proteins, which might be responsible for the stabilization of the nanoparticles [42].

**3.4. XRD.** The XRD pattern of the biosynthesized CdS nanoparticles (Figure 3) exhibited diffraction peaks at  $2\theta$  values of 26.33, 43.65, and 51.6 corresponding to the (111), (220), and (311) planes of CdSNP cubic phase (Joint Committee for Powder Diffraction Standards (JCPDS) 10-454). The occurrence of these broad peaks indicated that the particles either have very small sizes of crystallite or are semicrystalline in nature. The width of the XRD diffraction peaks was indicative of the relatively small particle size and heterogeneous particle size distribution [43].



(a)



[Measurement properties]  
 Wavelength range (nm.): 200.00 to 600.00  
 Scan speed: Fast  
 Sampling interval: 0.5  
 Autosampling interval: Enabled  
 Scan Mode: Single

No.	Wavelength	Absorbance	Description
1	273.00	1.306	
2	430.00	0.395	
3			

[Instrument properties]  
 Instrument type: UV-1800 series  
 Measuring mode: Absorbance  
 Slit width: 1.0 nm  
 Light source change wavelength: 340.0 nm  
 S/R exchange: Normal

[Attachment properties]  
 Attachment: None

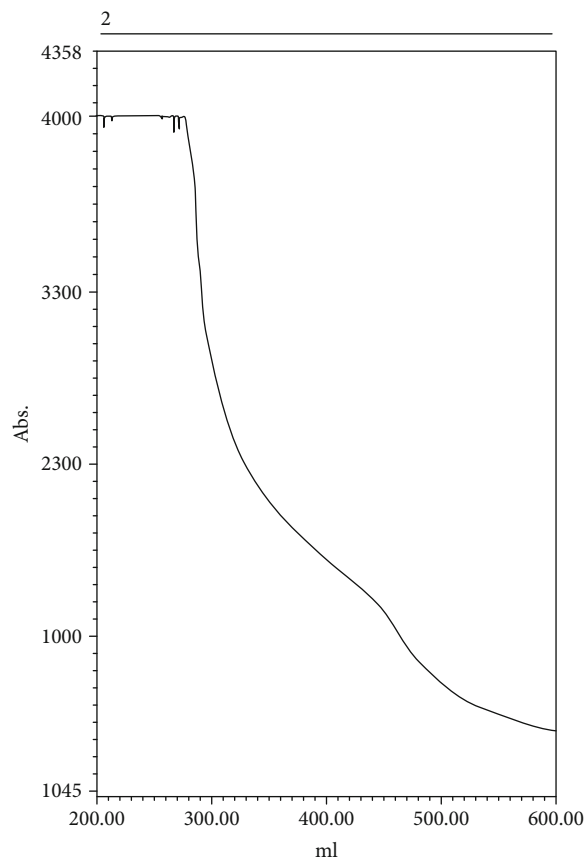
[Operation]  
 Threshold: 0.0010000  
 Points: 4  
 Interpolate: Disabled  
 Average: Disabled

(Sample preparation properties)  
 Weight:  
 Volume:  
 Dilution:  
 Path length:  
 Additional information:

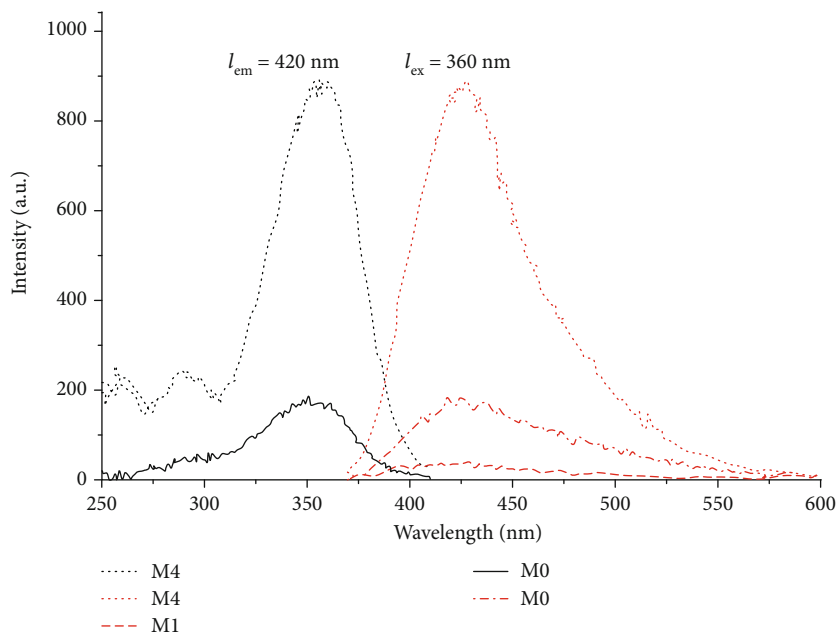
(b)

FIGURE 1: Continued.

No.	Wavelength	Absorbance	Description
1	445.50	1.153	



(c)



(d)

FIGURE 1: (a–c) Graphs of the UV-Vis scan: (a) sample incubated for three months; (b) photoluminescence spectra (c) of the cadmium sulfide nanoparticle biosynthesized by *Aspergillus niger* (RCMB 002002). (d) The surface plasmon excitation bands for cadmium sulfide nanoparticle biosynthesized by *Aspergillus niger* (RCMB 002002).

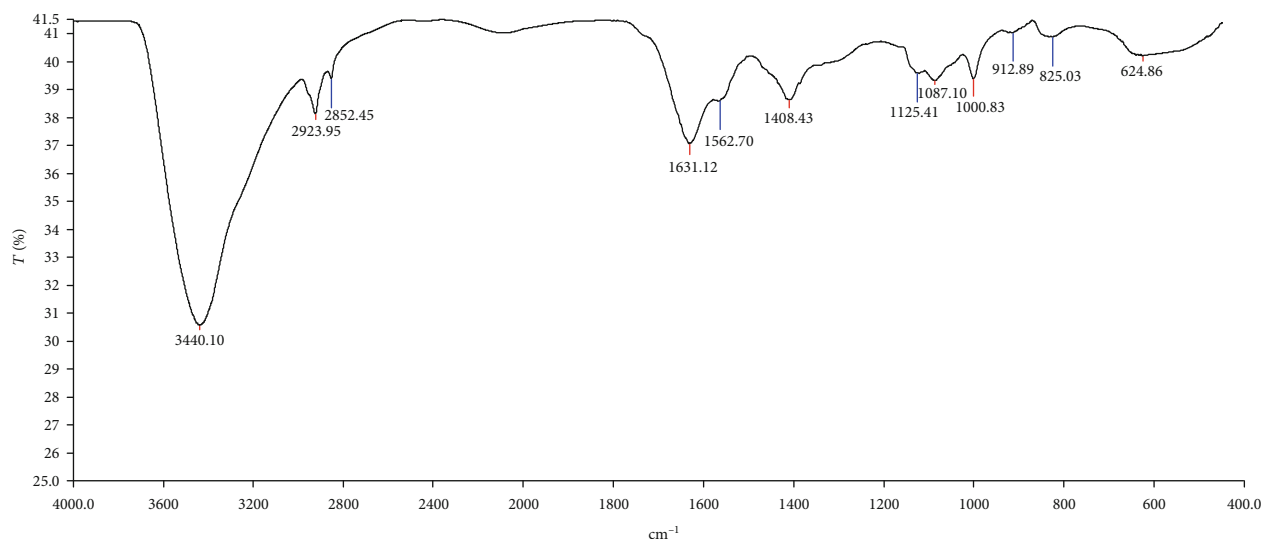


FIGURE 2: The FTIR spectrum of the cadmium sulfide nanoparticles biosynthesized by *Aspergillus niger* (RCMB 002002).

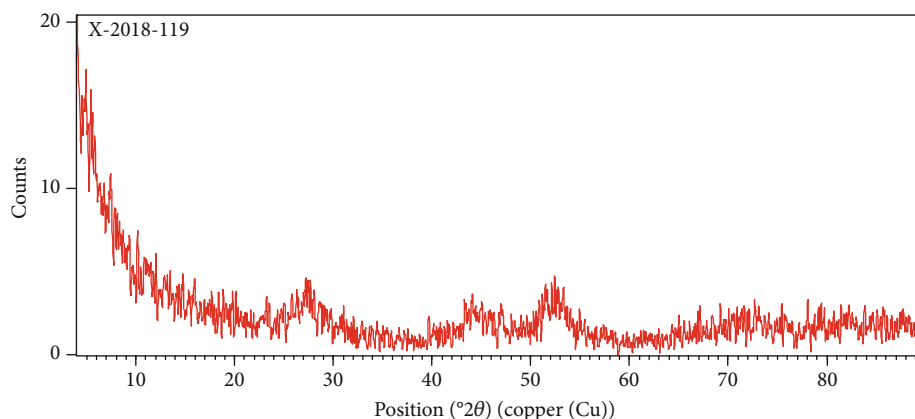


FIGURE 3: X-ray diffraction (XRD) pattern of the cadmium sulfide nanoparticles biosynthesized by *Aspergillus niger* (RCMB 002002). Start position ( $^{\circ}2\theta$ ): 4.0100; end position ( $^{\circ}2\theta$ ): 89.9900; step size ( $^{\circ}2\theta$ ): 0.0200; scan type: continuous; anode material: Cu-K-alpha1 ( $\text{\AA}$ ): 1.54060; generator settings: 40 mA, 40 kV.

**3.5. DLS.** Figure 4 shows the typical size and distribution of the biosynthesized CSNP size as tested by DLS. It can be observed that 100% of the CSNP size distribution falls within 2.7-7.5 nm range, thus displaying a unimodal size distribution. The particle sizes tested by DLS were significantly larger than those observed by the TEM, where the technique of DLS gives a mean of hydrodynamic diameter for CSNP core surrounded by the organic and solvation layers, and this hydrodynamic diameter is influenced by the viscosity and the concentration of the solution [44].

**3.6. TEM and EDX.** Figure 5 shows that the biologically stabilized nanosized particle cluster clearly had a polymeric pattern as uniform and fine particles, which form crystalline aggregates. As illustrated before, these protein molecules and the peptide molecules stabilized the generated nuclei of CdS and disallowed their extra growth [45]. According to these images, the regular size of the monodispersed

nanoparticles resulted to be within a range of 2–10 nm, and some larger particles might be due to the aggregation or smaller particle overlap. The clusters of CSNPs are formed by individual QDs separated through a thin, less electronically dense capping.

The CdS nanocrystallite biosynthesis displayed an optical absorption band that peaked at 3–4 keV (Figure 5), which is the typical absorption of metallic CdS nanocrystallites due to the surface plasmon resonance [10, 46]. The derived EDX spectrum also presented some peaks linked to the cadmium and sulfur elements, with the atomic weight fraction of the constituent elements reaching nearly 1 : 1 in the biosynthesized forms. These results are in agreement with those reported by El-Baz et al. [18].

**3.7. Cytotoxicity Assay.** Because of their distinctive properties, such as their tiny size, high surface-to-volume ratio, and slow release abilities, nanoparticles are considered to



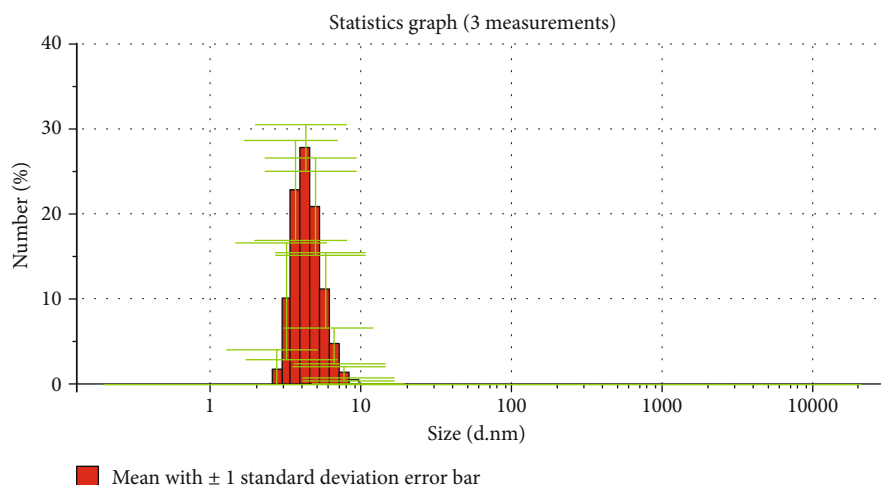


FIGURE 4: Particle size analysis of the cadmium sulfide nanoparticles biosynthesized by *Aspergillus niger* (RCMB 002002). Malvern Instruments Ltd., serial number: MAL1071664, Zetasizer ver. 6.32.

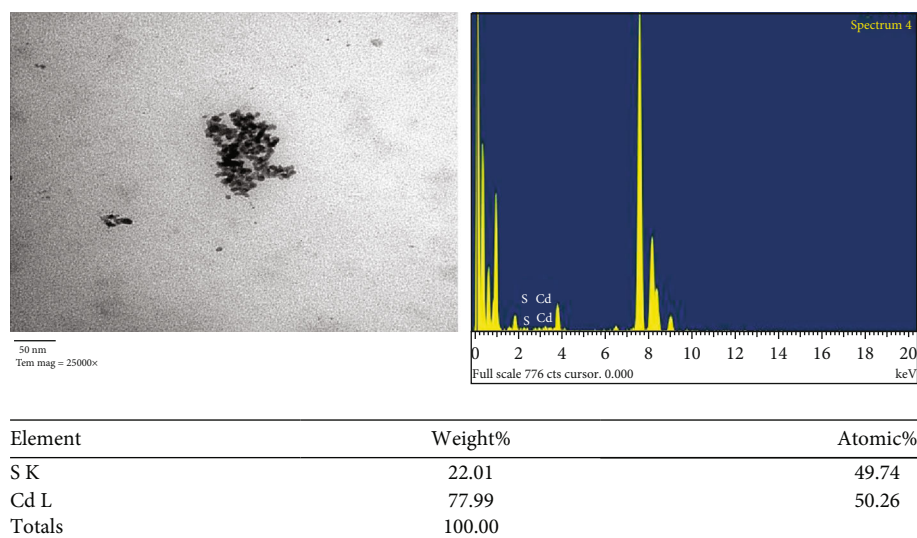


FIGURE 5: Transmission electron microscopy of the cadmium sulfide nanoparticles biosynthesized by *Aspergillus niger* (RCMB 002002).

possess enhanced cytotoxic potential [47]. To study the biosynthesized NP cytotoxicity, investigations against different cancer cell lines have been performed.

Figures 6(a)–6(c) show the cytotoxic effects of the CdSNPs against the MCF7, PC3, and A549 diseased cell lines of the cell growth, as examined by the MB assay at different concentrations (3.9, 7.8, 15.6, 31.25, 62.50, 125, 250, and 500  $\mu\text{g}/\text{mL}$ ). The inhibitory concentrations (IC50) of the CdSNPs were recorded at 190  $\mu\text{g}\cdot\text{mL}^{-1}$  against MCF7, 246  $\mu\text{g}\cdot\text{mL}^{-1}$  against PC3, and 149  $\mu\text{g}\cdot\text{mL}^{-1}$  against A549 cells.

Similarly, the inhibitory concentration (IC50) of phyto-mediated AgNPs was recorded at 60  $\mu\text{g}\cdot\text{mL}^{-1}$  against MCF7 and 50  $\mu\text{g}\cdot\text{mL}^{-1}$  against A549 cells [48], whereas Prasanna et al. [49] reported 400 mg of IC50 value against the MCF7 cancer cell line for the AuNPs which are prepared from the leaf extract of *Cassia auriculata*.

Exposing human prostate carcinoma cell line PC3 cells to a methanolic leaf extract of *Cordia dichotoma* (MECD) increased the cell death significantly ( $p < 0.001$ , IC50 = 74.5  $\mu\text{g}/\text{mL}$ ) [50]. This cell death might have occurred due to (i) the release of the interior cadmium ion ( $\text{Cd}^{+2}$ ) from CSNPs into the cell media, causing cell death, and/or (ii) reactive oxygen species (ROS) formation [51]. The release of cadmium ions from CSNPs into cell media leads to the surface oxidation of the CSNPs [52]. It has been postulated that chalcogenide atoms (Se, S) located on the surface of the Q-dots could be oxidized by oxygen molecules to form oxides ( $\text{SeO}_2$ ,  $\text{SO}_4^{2-}$ ):



In the case of CSNPs, the formed  $\text{SO}_4^{2-}$  molecules were

14 February 2018

Cytotoxicity report

14 February 2018

Cytotoxicity report

Al-Azhar University  
The Regional Center for Mycology&Biotechnology

Al-Azhar University  
The Regional Center for Mycology&Biotechnology

Evaluation of cytotoxicity against MCF-7 cell line

Evaluation of cytotoxicity against PC-3 cell line

Requester Data:

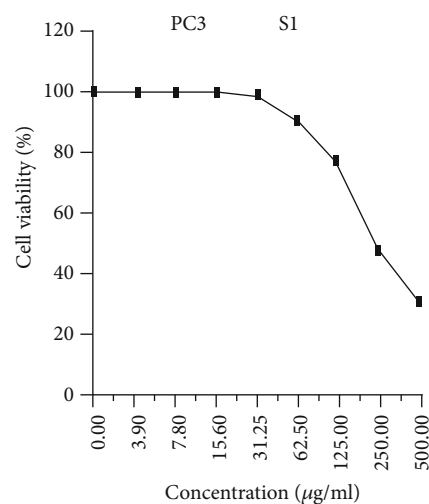
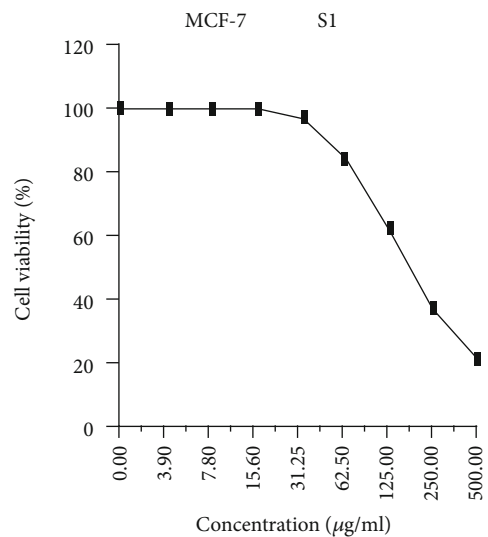
Name: Prof. Dr. Ashraf El-Baz  
Dr. Sherin Hesham

Requester Data:

Name: Prof. Dr. Ashraf El-Baz  
Dr. Sherin Hesham

Sample Code: (S<sub>1</sub>)

Sample Code: (S<sub>1</sub>)



Sample conc. (µg/ml)	Viability %	Inhibitory %	S.D. (±)
500	21.94	78.06	0.72
250	38.17	61.83	0.89
125	62.85	37.15	1.37
62.5	98.15	14.97	0.62
31.25	100	1.85	0.09
15.6	100	0	
7.8	100	0	
3.9	100	0	
0	100	0	

Sample conc. (µg/ml)	Viability %	Inhibitory %	S.D. (±)
500	32.78	67.22	0.94
250	49.06	50.94	1.86
125	78.13	21.87	1.98
62.5	92.44	7.56	0.38
31.25	99.78	0.22	0.12
15.6	100	0	
7.8	100	0	
3.9	100	0	
0	100	0	

Comment:

Inhibitory activity against Breast carcinoma cells was detected under these experimental conditions with IC<sub>50</sub>-19 0± 3.5 µg/ml.

Comment:

Inhibitory activity against Breast carcinoma cells was detected under these experimental conditions with IC<sub>50</sub>-246± 4.1 µg/ml.

(a)

(b)

FIGURE 6: Continued.



14 February 2018

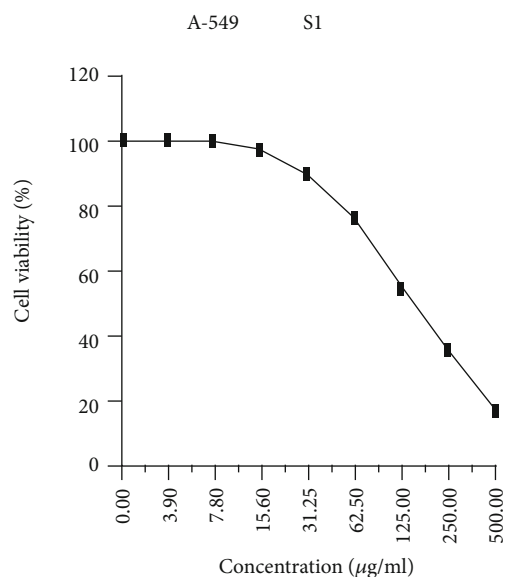
Cytotoxicity report

Al-Azhar University  
The Regional Center for Mycology&Biotechnology

Evaluation of cytotoxicity against A-549 cell line

Requester Data:

Name: Prof. Dr. Ashraf El-Baz  
Dr. Sherin Hesham

Sample Code: (S<sub>1</sub>)

Sample conc. (µg/ml)	Viability %	Inhibitory %	S.D. (±)
500	15.82	84.18	0.46
250	35.64	64.36	2.37
125	53.49	46.51	1.95
62.5	76.38	23.62	0.84
31.25	89.56	10.44	0.13
15.6	97.12	2.88	0.04
7.8	100	0	
3.9	100	0	
0	100	0	

Comment:

Inhibitory activity against Breast carcinoma cells was detected under these experimental conditions with IC<sub>50</sub>-149± 2.9 µg/ml.

(c)

FIGURE 6: *In vitro* cell cytotoxicity (MB assay) on the CdSNPs biosynthesized by *Aspergillus niger* (RCMB 002002) against the MCF7, PC3, and A549 diseased cell lines.

released from the surface, leaving behind “dangling” reduced Cd atoms [53]. Thus, prolonged CSNP exposure to an oxidative environment can cause the decomposition of CSNPs, thereby leading to the release of Cd ions.

3.8. *Antimicrobial Properties.* Since Klabunde and his coworkers demonstrated that the reactive of metal oxide nanoparticles displays strong antibacterial activity [54], there has been great interest in exploring the use of inorganic

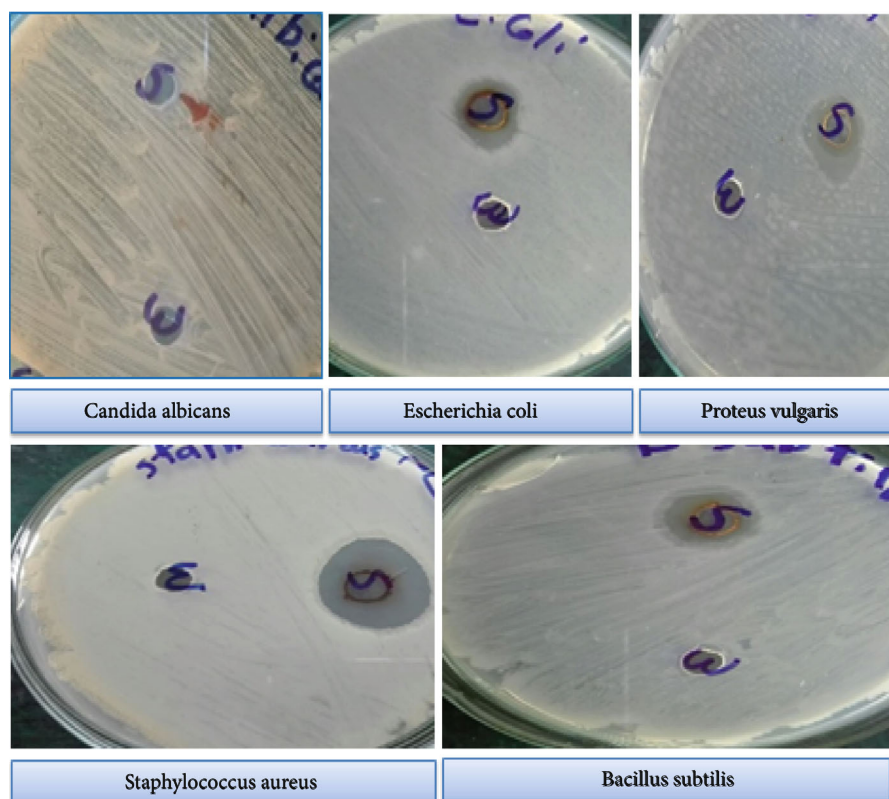


FIGURE 7: Antimicrobial activity of the biosynthesized CdSNPs against Gr<sup>+</sup> bacteria, Gr<sup>-</sup> bacteria, yeast, and fungi in comparison to gentamycin and ketoconazole.

TABLE 1: Antimicrobial activity of the biosynthesized CdS nanoparticles against Gr<sup>+</sup> bacteria, Gr<sup>-</sup> bacteria, yeast, and fungi in comparison to gentamycin and ketoconazole.

Tested microorganisms	Sample	Antimicrobial activity inhibition zone (mm)	
		Ketoconazole 100 $\mu\text{g}/\text{mL}$	Gentamycin 4 $\mu\text{g}/\text{mL}$
<i>Candida albicans</i> ATCC 10231	NA	20	
<i>Bacillus subtilis</i> NRRL B-543	16		26
<i>Staphylococcus aureus</i> RCMB010010	25		24
<i>Escherichia coli</i> ATCC 25955	14		30
<i>Proteus vulgaris</i> ATCC 13315	16		25

RCMB: Regional Center for Mycology and Biotechnology.

nanoparticles as antibacterial materials. The distinguishing characteristics of the inorganic nanoparticle materials have higher surface-to-volume ratios and their nanoscale extent, which enhance the combination with biological pathogens [55]. Figure 7 shows the antimicrobial activity of CdNPs against *Bacillus subtilis*, *Staphylococcus aureus*, *Escherichia coli*, *Proteus vulgaris*, and *Candida albicans*. It could be concluded that the CdNPs had a greater effect on the gram-positive bacteria than on the gram-negative ones, as indicated by the zone of inhibition (ZOI) values (Table 1), and the CdNPs presented significant antibacterial effect against all the examined bacterial pathogens. The lowest value is 16.0 mm (for both *Bacillus subtilis* and *P. vulgaris*), which is greater than the corresponding values given in many other studies [56, 57].

The difference in microorganism susceptibility might be attributed to the nature of the cell wall structure, which determines microorganism permeability. Lipopolysaccharides are present on the outer membrane of gram-negative bacteria, and they hinder the entrance of macromolecules and other hydrophilic molecules. By contrast, lipopolysaccharides are either present or absent in very minute quantities in gram-positive bacteria. In addition, these bacteria possess multiple peptidoglycan layers and negatively charged glycerin chains (teichoic acid) in their cell wall. Cadmium might disrupt the cell wall upon interaction with the negative charge of the cell wall. Mubarak Ali et al. reported that NPs could also affect the bacterial growth signaling pathway, thus interfering with the cell viability [58]. No antimicrobial action against *Candida albicans* was detected.

## 4. Conclusion

The results obtained from this study confirm that the cadmium-tolerant *Aspergillus niger* could be considered as an effective, low cost biological source for the biosynthesis of cadmium sulfide nanoparticles. These nanoparticles have antimicrobial and anticancer capabilities, and it could be a powerful tool for other biotechnological applications such as fluorescent microscopy and signal transduction. Also, 100% of the CSNPs measure from 2.7 to 7.5 nm, showing typical properties of QDs, such as emission spectra with a broad fluorescence peak at 420 nm and UV absorption onset at 430 nm. And these properties could favor its use in the fabrication of semiconductors when compared with those chemically synthesized.

## Data Availability

Data will be made available on request.

## Conflicts of Interest

The authors declare that they have no conflict of interest.

## References

- [1] P. Williams, E. Keshavarz-Moore, and P. Dunnill, "Efficient production of microbially synthesized cadmium sulfide quantum semiconductor crystallites," *Enzyme and Microbial Technology*, vol. 19, no. 3, pp. 208–213, 1996.
- [2] M. M. Borova, A. P. Naumenko, A. I. Yemets, and Y. B. Blume, "Stability of CdS quantum dots synthesized using *Escherichia coli* bacterium," *Reports of the National Academy of Sciences of Ukraine*, vol. 7, pp. 145–151, 2014.
- [3] K. B. Narayanan and N. Sakthivel, "Biological synthesis of metal nanoparticles by microbes," *Advances in Colloid and Interface Science*, vol. 156, no. 1–2, pp. 1–13, 2010.
- [4] J.-W. Moon, I. N. Ivanov, C. E. Duty et al., "Scalable economic extracellular synthesis of CdS nanostructured particles by a non-pathogenic thermophile," *Journal of Industrial Microbiology & Biotechnology*, vol. 40, no. 11, pp. 1263–1271, 2013.
- [5] P. R. Smith, J. D. Holmes, D. J. Richardson, D. A. Russell, and J. R. Sodeau, "Photophysical and photochemical characterisation of bacterial semiconductor cadmium sulfide particles," *Journal of the Chemical Society, Faraday Transactions*, vol. 94, no. 9, pp. 1235–1241, 1998.
- [6] R. Y. Sweeney, C. Mao, X. Gao et al., "Bacterial biosynthesis of cadmium sulfide nanocrystals," *Chemistry & Biology*, vol. 11, no. 11, pp. 1553–1559, 2004.
- [7] J. D. Holmes, P. R. Smith, R. Evans-Gowing, D. J. Richardson, D. A. Russell, and J. R. Sodeau, "Energy-dispersive X-ray analysis of the extracellular cadmium sulfide crystallites of *Klebsiella aerogenes*," *Archives of Microbiology*, vol. 163, no. 2, pp. 143–147, 1995.
- [8] H. J. Bai, Z. M. Zhang, Y. Guo, and G. E. Yang, "Biosynthesis of cadmium sulfide nanoparticles by photosynthetic bacteria *Rhodospseudomonas palustris*," *Colloids and Surfaces B: Biointerfaces*, vol. 70, no. 1, pp. 142–146, 2009.
- [9] D. P. Cunningham and L. L. Lundie Jr., "Precipitation of cadmium by *Clostridium thermoaceticum*," *Applied and Environmental Microbiology*, vol. 59, no. 1, pp. 7–14, 1993.
- [10] C. Malarkodi, S. Rajeshkumar, K. Paulkumar, G. G. Jobitha, M. Vanaja, and G. Annadurai, "Biosynthesis of semiconductor nanoparticles by using sulfur reducing bacteria *Serratia nematodiphila*," *Advances in Nano Research*, vol. 1, no. 2, pp. 83–91, 2013.
- [11] L. Wang, S. Chen, Y. Ding, Q. Zhu, N. Zhang, and S. Yu, "Biofabrication of morphology improved cadmium sulfide nanoparticles using *Shewanella oneidensis* bacterial cells and ionic liquid: for toxicity against brain cancer cell lines," *Journal of Photochemistry and Photobiology B: Biology*, vol. 178, pp. 424–427, 2018.
- [12] X. Li, S. Chen, W. Hu et al., "In situ synthesis of CdS nanoparticles on bacterial cellulose nanofibers," *Carbohydrate Polymers*, vol. 76, no. 4, pp. 509–512, 2009.
- [13] K. Prasad and A. K. Jha, "Biosynthesis of CdS nanoparticles: an improved green and rapid procedure," *Journal of Colloid and Interface Science*, vol. 342, no. 1, pp. 68–72, 2010.
- [14] S. Rajeshkumar, M. Ponnaniakamadeen, C. Malarkodi, M. Malini, and G. Annadurai, "Microbe-mediated synthesis of antimicrobial semiconductor nanoparticles by marine bacteria," *Journal of Nanostructure in Chemistry*, vol. 4, no. 2, p. 96, 2014.
- [15] K. Sahayaraj and S. Rajesh, "Bionanoparticles: synthesis and antimicrobial applications," *Science Against Microbial Pathogens: Communicating Current Research and Technological Advances*, vol. 23, pp. 228–244, 2011.
- [16] C. T. Dameron, B. R. Smith, and D. R. Winge, "Glutathione-coated cadmium- sulfide crystallites in *Candida glabrata*," *The Journal of Biological Chemistry*, vol. 264, no. 29, pp. 17355–17360, 1989.
- [17] N. Krumov, S. Oder, I. Perner-Nochta, A. Angelov, and C. Posten, "Accumulation of Cds nanoparticles by yeasts in a fed-batch bioprocess," *Journal of Biotechnology*, vol. 132, no. 4, pp. 481–486, 2007.
- [18] A. F. El-Baz, N. M. Sorour, and Y. M. Shetaia, "Trichosporon jirovecii-mediated synthesis of cadmium sulfide nanoparticles," *Journal of Basic Microbiology*, vol. 56, no. 5, pp. 520–530, 2016.
- [19] R. Wu, C. Wang, J. Shen, and F. Zhao, "A role for biosynthetic CdS quantum dots in extracellular electron transfer of *Saccharomyces cerevisiae*," *Process Biochemistry*, vol. 50, no. 12, pp. 2061–2065, 2015.
- [20] A. Ahmad, P. Mukherjee, D. Mandal et al., "Enzyme mediated extracellular synthesis of CdS nanoparticles by the fungus *Fusarium oxysporum*," *Journal of the American Chemical Society*, vol. 124, no. 41, pp. 12108–12109, 2002.
- [21] L. Reyes, I. Gomez, and M. T. Garza, "Biosynthesis of cadmium sulfide nanoparticles by the fungi *Fusarium* sp.," *International Journal of Nanotechnology: Biomedicine*, vol. 1, no. 1, pp. 90–95, 2009.
- [22] I. Sandoval-Cárdenas, M. Gómez-Ramírez, and N. G. Rojas-Avelizapa, "Use of a sulfur waste for biosynthesis of cadmium sulfide quantum dots with *Fusarium oxysporum* f. sp. lycopersici," *Materials Science in Semiconductor Processing*, vol. 63, pp. 33–39, 2017.
- [23] A. S. Bhadwal, R. M. Tripathi, R. K. Gupta, N. Kumar, R. P. Singh, and A. Shrivastav, "Biogenic synthesis and photocatalytic activity of CdS nanoparticles," *RSC Advances*, vol. 4, no. 19, pp. 9484–9490, 2014.
- [24] M. Borovaya, Y. Pirko, T. Krupodorova, A. Naumenko, Y. Blume, and A. Yemets, "Biosynthesis of cadmium sulphide

- quantum dots by using *Pleurotus ostreatus* (Jacq.) P. Kumm," *Biotechnology and Biotechnological Equipment*, vol. 29, no. 6, pp. 1156–1163, 2015.
- [25] G. Chen, B. Yi, G. Zeng et al., "Facile green extracellular biosynthesis of CdS quantum dots by white rot fungus *Phanerochaete chrysosporium*," *Colloids and Surfaces B: Biointerfaces*, vol. 117, pp. 199–205, 2014.
- [26] R. Sanghi and P. Verma, "A facile green extracellular biosynthesis of CdS nanoparticles by immobilized fungus," *Chemical Engineering Journal*, vol. 155, no. 3, pp. 886–891, 2009.
- [27] B. A. Rzigalinski and J. S. Strobl, "Cadmium-containing nanoparticles: perspectives on pharmacology and toxicology of quantum dots," *Toxicology and Applied Pharmacology*, vol. 238, no. 3, pp. 280–288, 2009.
- [28] A. Azam, A. S. Ahmed, M. Oves, M. S. Khan, S. S. Habib, and A. Memic, "Antimicrobial activity of metal oxide nanoparticles against Gram-positive and Gram-negative bacteria: a comparative study," *International Journal of Nanomedicine*, vol. 7, pp. 6003–6009, 2012.
- [29] T. Mosmann, "Rapid colorimetric assay for cellular growth and survival application to proliferation and cytotoxicity assays," *Journal of Immunological Methods*, vol. 65, no. 1–2, pp. 55–63, 1983.
- [30] J. Virkutyte and R. S. Varma, "Green synthesis of metal nanoparticles: biodegradable polymers and enzymes in stabilization and surface functionalization," *Chemical Science*, vol. 2, no. 5, pp. 837–846, 2011.
- [31] Y. B. Blume, Y. V. Pirko, O. M. Burlaka et al., "«Green» synthesis of noble metal nanoparticles and CdS Semiconductor nanocrystals using biological materials," *Science and Innovation*, vol. 11, no. 1, pp. 55–66, 2015.
- [32] Z. R. Khan, M. Zulfeqar, and M. S. Khan, "Chemical synthesis of CdS nanoparticles and their optical and dielectric studies," *Journal of Materials Science*, vol. 46, no. 16, pp. 5412–5416, 2011.
- [33] A. L. Pan, J. G. Ma, X. Z. Yan, and B. S. Zou, "The formation of CdS nanocrystals in silica gels by gamma-irradiation and their optical properties," *Journal of Physics: Condensed Matter*, vol. 16, no. 18, pp. 3229–3238, 2004.
- [34] L. E. Brus, "Electron-electron and electron-hole interactions in small semiconductor crystallites: the size dependence of the lowest excited electronic state," *The Journal of Chemical Physics*, vol. 80, no. 9, pp. 4403–4409, 1984.
- [35] R. Bhattacharya and S. Saha, "Growth of Cds nanoparticles by chemical method and its characterization," *Pramana*, vol. 71, no. 1, pp. 187–192, 2008.
- [36] S. Tandon and S. Vats, "Microbial biosynthesis of cadmium sulfide (CDS) nanoparticles and their characterization," *European Journal of Pharmaceutical and Medical Research*, vol. 3, no. 9, pp. 545–550, 2016.
- [37] M. D. Rao and G. Pennathur, "Green synthesis and characterization of cadmium sulphide nanoparticles from *Chlamydomonas reinhardtii* and their application as photocatalysts," *Materials Research Bulletin*, vol. 85, pp. 64–73, 2017.
- [38] R. A. Mousavi, A. A. Sepahy, and M. R. Fazeli, "Biosynthesis, purification and characterization of cadmium sulfide nanoparticles using Enterobacteriaceae and their application," in *Proceedings of the International Conference Nanomaterials: Applications and Properties 1:5*, Sumy State University, Alushta, The Crimea, Ukraine Kindly refer, 2012.
- [39] R. Bhambure, M. Bule, N. Shaligram, M. Kamat, and R. Singhal, "Extracellular biosynthesis of gold nanoparticles using *Aspergillus niger* - its characterization and stability," *Chemical Engineering and Technology*, vol. 32, no. 7, pp. 1036–1041, 2009.
- [40] Y. Xia and N. J. Halas, "Shape-controlled synthesis and surface plasmonic properties of metallic nanostructures," *MRS Bulletin*, vol. 30, no. 5, pp. 338–348, 2005.
- [41] Y. Wang, G. Meng, L. Zhang, C. Liang, and J. Zhang, "Catalytic growth of large-scale single crystal CdS nanowires by physical evaporation and their photoluminescence," *Chemistry of Materials*, vol. 14, no. 4, pp. 1773–1777, 2002.
- [42] X. Zhu, D. Kumari, M. Huang, and V. Achal, "Biosynthesis of CdS nanoparticles through microbial induced calcite precipitation," *Materials and Design*, vol. 98, pp. 209–214, 2016.
- [43] H. P. Klug and L. E. Alexander, *X-Ray Diffraction Properties for Polycrystalline and Amorphous Materials*, Wiley, New York, 1974.
- [44] Y. L. Wu, C. S. Lim, S. Fu et al., "Surface modifications of ZnO quantum dots for bio-imaging," *Nanotechnology*, vol. 18, no. 21, p. 215604, 2007.
- [45] A. Sankhla, R. Sharma, R. S. Yadav, D. Kashyap, S. L. Kothari, and S. Kachhwaha, "Biosynthesis and characterization of cadmium sulfide nanoparticles – an emphasis of zeta potential behavior due to capping," *Materials Chemistry and Physics*, vol. 170, pp. 44–51, 2016.
- [46] S. R. K. Pandian, V. Deepak, K. Kalishwaralal, and S. Gurunathan, "Biologically synthesized fluorescent CdS NPs encapsulated by PHB," *Enzyme and Microbial Technology*, vol. 48, no. 4–5, pp. 319–325, 2011.
- [47] D. Wang, Z. Lin, T. Wang et al., "Where does the toxicity of metal oxide nanoparticles come from: the nanoparticles, the ions, or a combination of both?," *Journal of Hazardous Materials*, vol. 308, pp. 328–334, 2016.
- [48] K. Venugopal, H. A. Rather, K. Rajagopal et al., "Synthesis of silver nanoparticles (Ag NPs) for anticancer activities (MCF 7 breast and A549 lung cell lines) of the crude extract of *Syzygium aromaticum*," *Journal of Photochemistry and Photobiology B: Biology*, vol. 167, pp. 282–289, 2017.
- [49] R. Prasanna, C. Harish, R. Pichai, D. Sakthisekaran, and P. Gunasekaran, "Anti-cancer effect of *Cassia auriculata* leaf extract in vitro through cell cycle arrest and induction of apoptosis in human breast and larynx cancer cell lines," *Cell Biology International*, vol. 33, no. 2, pp. 127–134, 2009.
- [50] M. A. Rahman and J. A. Sahabjada, "Evaluation of anticancer activity of *Cordia dichotoma* leaves against a human prostate carcinoma cell line, PC3," *Journal of Traditional and Complementary Medicine*, vol. 7, no. 3, pp. 315–321, 2017.
- [51] D. Maysinger, J. Lovric, A. Eisenberg, and R. Savic, "Fate of micelles and quantum dots in cells," *European Journal of Pharmaceutical and Biopharmaceutics*, vol. 65, no. 3, pp. 270–281, 2007.
- [52] A. M. Derfus, W. C. W. Chan, and S. N. Bhatia, "Probing the cytotoxicity of semiconductor quantum dots," *Nano Letters*, vol. 4, no. 1, pp. 11–18, 2004.
- [53] K. M. K. Selim, I.-K. Kang, and H. Guo, "Albumin-conjugated cadmium sulfide nanoparticles and their interaction with KB cells," *Macromolecular Research*, vol. 17, no. 6, pp. 403–410, 2009.
- [54] K. J. Klabunde, J. Stark, O. Koper et al., "Nanocrystals as stoichiometric reagents with unique surface chemistry," *The*

- Journal of Physical Chemistry*, vol. 100, no. 30, pp. 12142–12153, 1996.
- [55] Z.-m. Xiu, Q.-b. Zhang, H. L. Puppala, V. L. Colvin, and P. J. J. Alvarez, “Negligible particle-specific antibacterial activity of silver nanoparticles,” *Nano Letters*, vol. 12, no. 8, pp. 4271–4275, 2012.
- [56] B. Buszewski, V. Railean-Plugaru, P. Pomastowski et al., “Antimicrobial activity of biosilver nanoparticles produced by a novel *Streptacidiphilus durhamensis* strain,” *Journal of Microbiology, Immunology, and Infection*, vol. 51, no. 1, pp. 45–54, 2018.
- [57] M. S. Abdel-Aziz, M. S. Shaheen, A. A. El-Nekeety, and M. A. Abdel-Wahhab, “Antioxidant and antibacterial activity of silver nanoparticles biosynthesized using *Chenopodium murale* leaf extract,” *Journal of Saudi Chemical Society*, vol. 18, no. 4, pp. 356–363, 2014.
- [58] D. MubarakAli, N. Thajuddin, K. Jeganathan, and M. Gunasekaran, “Plant extract mediated synthesis of silver and gold nanoparticles and its antibacterial activity against clinically isolated pathogens,” *Colloids and Surfaces B: Biointerfaces*, vol. 85, no. 2, pp. 360–365, 2011.